DOI:10.1190/1.3255106

Conventional versus dual-sensor streamer data de-ghosting; A case study from the Haltenbanken dual-streamer acquisition.

Hocine Tabti, Anthony Day, Terry Schade, Marina Lesnes and Torben Høy, PGS*

Summary

Recent developments in the field of marine towed streamer acquisition technologies have brought about new data information that needs to be assessed and compared to conventional data. Dual-sensor towed streamer acquisition, with its wave-field decomposition capabilities, is one such recent development. The present work compares conventional data with dual-sensor data acquired simultaneously at 2 different depths. The two streamers were towed vertically under each other, the conventional at 8m depth and the dual-sensor at 15m depth. To facilitate comparison the data from the two streamers have been processed optimally and in the same manner, i.e. wave field decomposition was also conducted on the conventional streamer data. The resulting up-going pressure field was compared to the up-going pressure field derived from the dual-sensor data. The comparison shows a clear advantage for the dual-sensor wave field decomposition result. Since the comparison is mostly limited to the low frequencies in this case, the superior result from the dual-sensor streamer data is attributed to better signal-to-noise ratio due to a deeper towing depth.

Introduction

The Haltenbanken dual streamer data was acquired in 2007 on the mid-Norwegian continental shelf in the Norwegian Sea. The objectives are at various prospective target depths in a deep and relatively complex structural and stratigraphic geological setting in which both resolution and depth of penetration are an issue.

The 2D acquisition geometry consisted of two spatially coincident streamers towed vertically above each other. A conventional hydrophone-only streamer was towed at 8m depth below sea-level whereas a dual-sensor streamer was towed below it at 15m depth. The common source was towed at 7m depth. Two lines of data were acquired using this geometry on the same prospect. The location of the two lines ("seq1" and "seq2") is indicated in Figure 1. This dataset presents an opportunity to compare the performance of the dual-sensor streamer with a conventional streamer under varied acquisition conditions.

A dual-sensor streamer records both pressure and the vertical component of particle velocity with collocated sensors allowing for very efficient decomposition of the wave-field into up- and down-going components at the receiver locations. This operation is often called (receiver-side) de-ghosting. This procedure and the consequent data quality enhancements have been demonstrated in several publications (e.g. Carlson et al., 2007; Long et al., 2008).

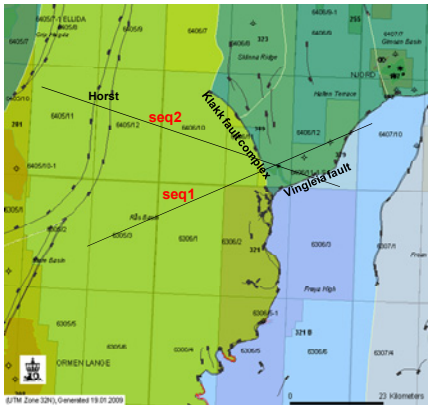

Figure 1. *Location of the two lines*

In this paper we address the question of de-ghosting the conventional hydrophone-only data by applying the same wave-field decomposition method that is done for the dual-sensor data (cf. Amundsen, 1993), which facilitates comparison of the datasets. Seq1, which was acquired in varied weather conditions (marginal at the start of the line, calming out towards the end of the line), is used for that purpose. This comparison further demonstrates the superiority of dual-sensor acquisition.

Pre-processing and wave-field decomposition

The theory behind wave-field decomposition has been described by a number of authors, e.g. Amundsen (1993); Fokkema and van den Berg (1993). Below is a brief description of the pre-processing steps that allow us to decompose data into up- and down-going components at the receiver locations.

When the vertical component of the particle velocity wave-field is coincidently measured along with the pressure wave-field, the two components can be used directly to decompose the total wave-fields into their up- and down-going components. For the pressure wave-field the two components are given as:

$$P^{up} = \frac{1}{2}\left(P - FV_z\right) \quad \text{and} \quad P^{down} = \frac{1}{2}\left(P + FV_z\right). \qquad (1)$$

P is the measured total pressure wave-field, V_z is the measured vertical component of the total particle velocity wave-field and F is an angle-dependent scaling factor. In

DOI:10.1190/1.3255106

the frequency wave number domain, the scaling filter F is (Amundsen, 1993):

$$F(\omega,k_x,k_y)=\frac{\rho\omega}{k_z},\quad \text{with}\quad k_z=\sqrt{\left(\frac{\omega}{v_w}\right)^2-k_x^2-k_y^2}\,. \qquad (2)$$

where k_x, k_y and k_z denote the three components of the angular wave-number vector, ω denotes angular frequency, and ρ and v_w are the density of water and the acoustic wave propagation velocity in water, respectively.

However, in practice, the recorded high frequency vertical particle velocity is merged with the low frequency portion of the vertical particle velocity which is rebuilt from the pressure record using the frequency-wave-number solution of the equation of motion (Tenghamn et al., 2007):

$$V_Z(\omega,k_x,k_y,z)=-\frac{k_z}{\rho\omega}\left[\frac{1+\exp(-2ik_z z)}{1-\exp(-2ik_z z)}\right]P(\omega,k_x,k_y,z), \qquad (3)$$

where z is the receiver depth. Notice that using equation (3) along with equation (1), one can in theory decompose conventional hydrophone-only data into up- and down-going components assuming a flat sea-surface with -1 reflection coefficient. The only limitation is that equation (3) cannot be used (is singular) at the ghost-notch frequencies of the hydrophone data. In practice, wave-field decomposition using only the hydrophone is flawed from sea-surface variations and noise content.

Processing and results

Identical processing flows were applied to data acquired by each of the two streamers. The main processing steps included noise-suppression both in x-t and τ-p domains, water-bottom gapped deconvolution on common receiver gathers after minimum phase conversion, surface-related multiple elimination (SRME) and finally Kirchhoff pre-stack time migration. The only difference for the dual-sensor data and the conventional hydrophone-only data is the wave-field separation step described previously and performed right after the noise suppression step above.

Figure 2 shows a comparison between the final migrated stack of the conventional total pressure (hydrophone) data without wave field decomposition and the same stack for the up-going pressure field obtained from the dual-sensor data. The figure shows some of the intermediate to deep prospective targets. Notice the superior illumination and resolution of the processed dual-sensor data.

Even though the dual-sensor data shows superior imaging capabilities it remains difficult to draw clear conclusions as we are attempting to compare two sections with completely different signal characteristics. One section (the dual-sensor data) contains de-ghosted signal with only the up-going pressure wave-field, whereas the other section (from the conventional hydrophone data) contains both the primary (up-going signal) and its ghost reflected from the sea-surface. In short this is not a fair comparison. In addition, most of the improvements in the deep section, as shown on the amplitude spectra of Figure 2, come from the very low frequencies where hydrophone-only signal was used in the wave-field decomposition as explained previously (i.e. using equations 3 and 1). The question arises: could we obtain a similar result if we use the same equations to de-ghost the conventional hydrophone-only data?

It has to be stressed however that the dual-sensor wave-field decomposition's use of the pressure-sensor signal is limited to very low frequencies where the motion sensors are relatively noisy whereas a wave-field decomposition of the conventional hydrophone-only data will make use of the hydrophone data (the only available) at all frequencies up to the vicinity of the second hydrophone notch. Figure 3 shows the hydrophone ghost functions for both 8m and 15m tow depth, which shows that for 8m tow depth the second hydrophone notch is at ~94Hz. Hence, for the hydrophone-only streamer we must filter out everything above 90Hz.

From inspection of Figure 3 it is clear that, if the noise level is identical at the two recording depths, the 15m tow depth will provide higher S/N ratio than 8m tow depth at the lowest frequencies for which the de-ghosted pressure field is derived solely from the hydrophone data in both cases. However, in practice the conventional streamer is subject to more swell in marginal weather due to its shallower tow depth of 8m compared to the relatively quieter conditions at 15m where the dual-sensor streamer is towed. This fact is illustrated on Figure 4 where average amplitude spectra calculated from start-of-the-line noise records are compared. The noise records were acquired simultaneously on the two streamers at the beginning of seq1 under marginal weather conditions. Towing deeper under such conditions is clearly advantageous. The lower noise level, combined with the enhanced signal illustrated in Figure 3, means that the S/N ratio at 15m tow depth is significantly better than at 8m for low frequencies. If a conventional hydrophone-only streamer were towed at 15m depth to take advantage of the quieter recording conditions, the usable seismic bandwidth would be restricted by the second hydrophone notch at about 50Hz. This would have an adverse impact on resolution, especially for the shallower targets. By using a dual-sensor streamer, data at the hydrophone notch frequencies is provided by the complementary signal recorded by the particle velocity sensor.

Figure 5 shows the same migrated stacks for seq1 as in Figure 2 but where both the conventional and dual-sensor data have been de-ghosted. This figure shows that the

DOI:10.1190/1.3255106

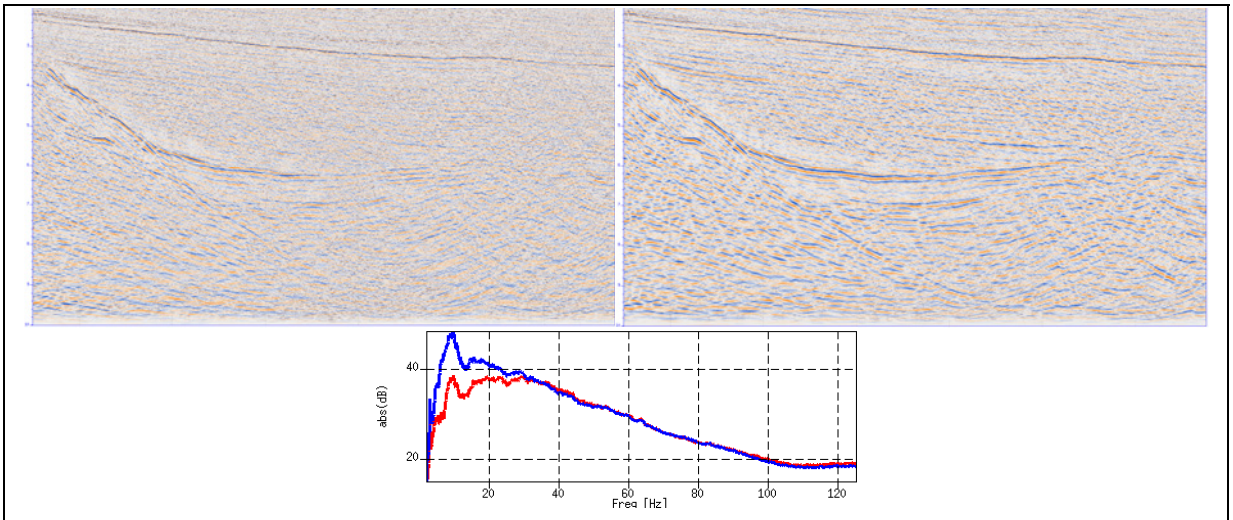

Figure 2: Final migrated stacks (seq1). Left: conventional hydrophone data. Right: up-going pressure data from dual-sensor. Bottom: corresponding average amplitude spectra (red: conventional; blue: dual-sensor)

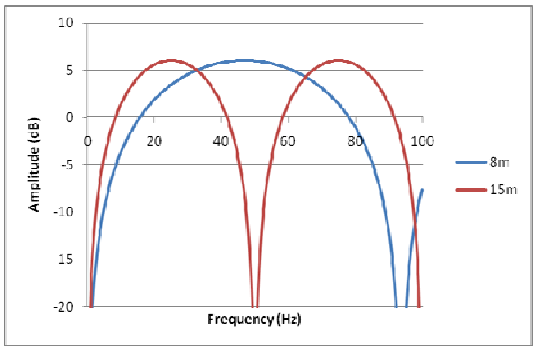

Figure 3: Ghost functions for 8m and 15m tow depth.

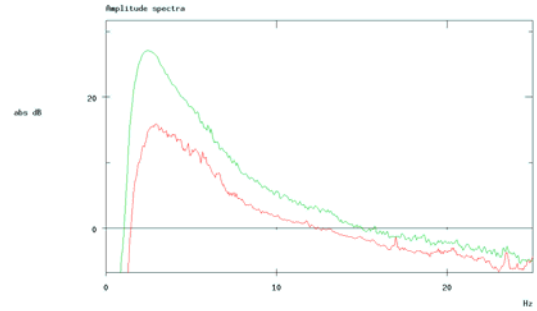

Figure 4: Average noise spectra (seq1). Green: conventional hydrophone noise (streamer towed at 8m depth). Red: dual-sensor hydrophone noise (streamer towed at 15m depth).

superior image quality observed in Figure 2 is maintained after de-ghosting of both datasets. The amplitude spectra of the two sections are now more similar except at the very low and very high frequencies. The effect of this processing sequence is to shape the signal recorded by both the dual-sensor and conventional streamers to the most desirable wavelet, i.e. a receiver-side deghosted signature, in a deterministic manner. However, the S/N ratio at any given frequency is unchanged. Hence the spectral discrepancies represent differences in the noise recorded by the two streamers. These discrepancies are observed near the notches in the hydrophone spectrum at 8m depth as shown in Figure 3, and are thus consistent with the preceding discussion of signal and noise recorded by the two streamers.

Another issue is the effect of the variable sea-surface on the ghost reflections. Wave-field decomposition of a conventional hydrophone-only streamer data assumes a flat sea-surface with -1 reflection coefficient. Both assumptions will be violated when the sea-surface shape is not flat.

The amplitude and phase of the ghost reflections will vary in a complicated and time-variant manner depending on the wave heights and wave lengths above the receiver locations. Furthermore the effect of sea-surface variations is frequency dependent, getting progressively worse towards higher frequencies. This is problematic for the conventional hydrophone-only streamer data de-ghosting where the entire frequency range has to be predicted as explained above.

Figure 6 shows one result from a finite-difference modeling study where sea-surface effects on the recorded signal were investigated. Receiver arrays were located 15m below average sea level. The source-side ghost variations are not included in the modeling. The plot to the right shows superimposed amplitude spectra of the reference signal (i.e.

DOI:10.1190/1.3255106

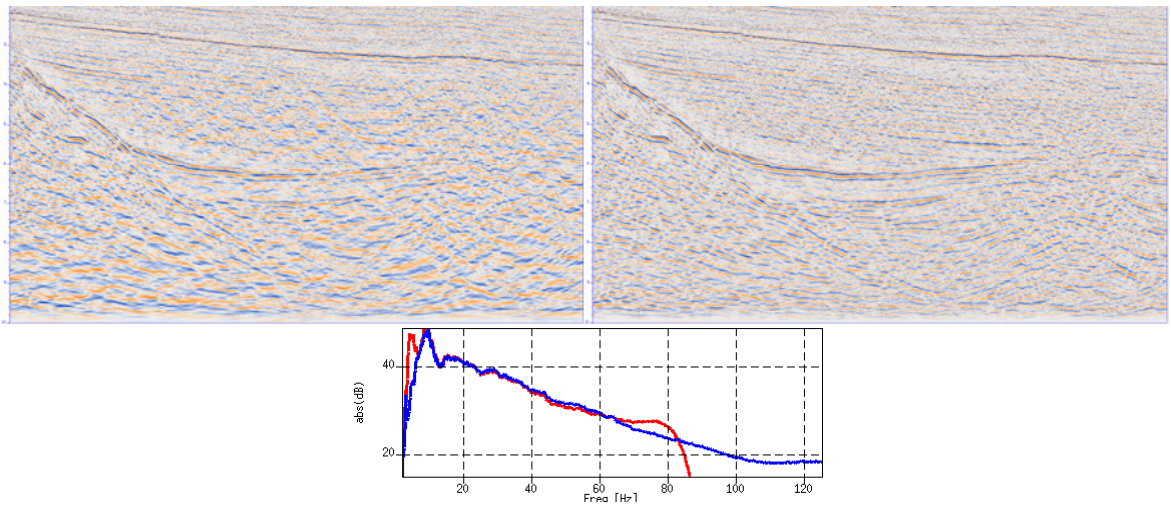

Figure 5: Final migrated stacks (seq1). Left: conventional de-ghosted up-going pressure data. Right: up-going pressure data from dual-sensor. Bottom: corresponding average amplitude spectra (red: conventional; blue: dual-sensor).

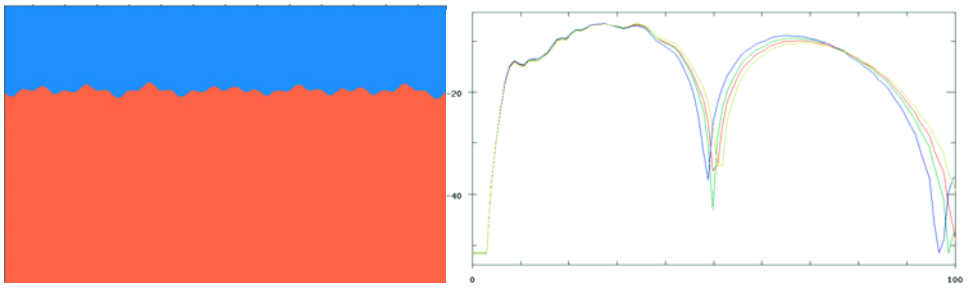

Figure 6: Finite-difference modeling of sea-surface effects. Left: section of one instance of water-air surface showing wave shapes. Right: superimposed amplitude spectra corresponding to modeled hydrophone signal for the reference (flat-sea) case (curve in red) and 3 other modeled signals with varied sea-surface shapes.

flat sea) and three other modeled signals from sea-surface shapes with 2m wave height (peak to average sea level) and 120m wave length. One instance of the wave shapes are shown on the left plot. Notice the progressive divergence of the curves as frequency increases. However, the flat-sea assumption clearly holds within the range of frequency replacement used in the dual-sensor data de-ghosting (up to 20Hz).

Conclusions

We have compared the final image quality for data acquired using a conventional hydrophone-only streamer towed at 8m depth to data contemporaneously acquired with a dual-sensor streamer towed vertically below at 15m depth. To facilitate this comparison, the conventional data were de-ghosted up to the second hydrophone notch frequency to provide a signal that is directly comparable with the up-going pressure field obtained from standard dual-sensor streamer processing. Under varied weather conditions, the dual-sensor streamer gives clearly superior image quality. This advantage comes from the signal enhancement that follows from the greater towing depth due to the comparative shape of the ghost function for different depths, and also because it is subjected to reduced levels of weather-related noise due to greater towing depth. Towing a conventional hydrophone cable at a similar depth is not a viable proposition without severely compromising the usable seismic bandwidth and consequently resolution.

Acknowledgments

We thank the crew of Ramform Explorer who acquired the data shown here and the many colleagues within PGS for their assistance and contributions. We thank PGS for permission to publish this data.

EDITED REFERENCES

Note: This reference list is a copy-edited version of the reference list submitted by the author. Reference lists for the 2009 SEG Technical Program Expanded Abstracts have been copy edited so that references provided with the online metadata for each paper will achieve a high degree of linking to cited sources that appear on the Web.

REFERENCES

Amundsen, L. ,1993, Wavenumber-based filtering of marine point-source data. Geophysics, **58**, 1335–1348.

Carlson, D., A. Long, W. Söllner, H. Tabti, R. Tenghamn, and N. Lunde, 2007, Increased resolution and penetration from a towed dual-sensor streamer: First Break, **25**, 71–77.

Fokkema, J. T., and P. M. van den Berg, 1993, Seismic applications of acoustic reciprocity: Elsevier.

Long, A., D. Mellors, T. Allen, and A. McIntyre, 2008, A calibrated dual-sensor streamer investigation of deep target signal resolution and penetration on the NW Shelf of Australia. 78th Annual International Meeting, SEG, Expanded Abstract, 428-432.

Tenghamn, R., S. Vaage, and C. Borresen, 2007, A dual-sensor towed marine streamer; its viable implementation and initial results: 77th Annual International Meeting, SEG, Expanded Abstract, 989–993.

DOI:10.1190/1.3255106